

# Synchrotron-Based FTIR Micro-spectroscopy of Martian Meteorites

*Araştırma Makalesi / Research Article*

**Mehmet YESILTAS\***

Kirklareli University, Faculty of Aeronautical and Space Sciences, Kirklareli, Turkey

(Received : 12.07.2017 ; Accepted : 15.08.2017)

## ÖZ

SNC grubundan Mars meteoritleri  $\sim 1 \mu\text{m}$  yüzeyel çözünürlüklü sinkrotron-tabanlı FTIR spektroskopisi ile orta-kızılötesi alanda incelendi (4000-850  $\text{cm}^{-1}$ ). EET A79001, ALH 84001, ve Nakhla meteoritlerinde silikat aralığı belirgin üç bandı ortaya koyarken, Chassigny farklı bir spektral profile sahiptir. Örneklerden bazılarının alifatik tip organik moleküller ve OH içerdiği kızılötesi spektra ile gösterilmiştir. Yüzeysel olarak çözümlenen dağılım haritalarında bu moleküllerin örnekler içinde heterojen olarak dağıldıkları görülmektedir. Bu durum ana-cisimde kompleks süreçlere işaret etmektedir.

**Anahtar Kelimeler:** Kızılötesi spektroskopisi, sinkrotron-ışınımı, meteoritler, mars, organikler.

# Synchrotron-Based FTIR Micro-spectroscopy of Martian Meteorites

## ABSTRACT

Martian meteorites from SNC group were studied with synchrotron-based FTIR spectroscopy with  $\sim 1 \mu\text{m}$  spatial resolution in the mid-infrared region (4000-850  $\text{cm}^{-1}$ ). Silicate region in EET A79001, ALH 84001, and Nakhla present three prominent bands, while Chassigny has a different spectral profile. The infrared spectra reveal that some of the grains contain aliphatic type organic molecules as well as OH. According to the spatially resolved distribution maps, these molecules appear to be heterogeneously distributed in the samples. This points to complex parent body processes.

**Keywords:** Infrared spectroscopy, synchrotron-radiation, meteorites, martian, organics.

## 1. INTRODUCTION

Martian meteorites originate from the planet Mars as a result of collisions between various bodies and the surface of Mars. Martian meteorites recovered on Earth consist of shergottite, nakhlite, and chassignite meteorites (SNCs), which have different chemical, mineralogical, elemental compositions [1]. The shergottites include subgroups of basaltic, olivine-phyric, and lherzolitic meteorites [2], and the distinction is based on their chemistry as well as textures [3]. In addition to SNCs, the martian meteorite collection also includes an orthopyroxenite sample Allan Hills 84001 (ALH 84001) [2], in which signatures of ancient martian life may have been [4]. Several spectroscopic methods have been used to study martian meteorites in the laboratory. For instance, Raman spectroscopy was used by [5] in order to investigate carbonate globules in ALH 84001. [6] used Mossbauer spectroscopy to interpret remote sensing data from Mars. In addition, x-ray spectroscopy was used to understand chemistry of phyllosilicates and sulfates on Mars [7]. Infrared spectroscopy is a particularly helpful technique for the study of martian meteorites [e.g., 8, 9, 10, 11, 12]. It was shown by [13] that synchrotron-based Fourier Transform infrared spectroscopy (FTIR) is able

to resolve organic and inorganic features in meteorites with  $\sim 1 \mu\text{m}$  spatial resolution.

Martian rocks provide a record of Mars's evolution [9]. Composition of Mars has been studied mostly through remote sensing techniques where an orbiter collects data from the surface of the Mars, although with a much larger pixel size. Future samples return missions to Mars will potentially provide pristine martian samples for study, until then martian meteorites recovered on Earth are the best possible martian samples to study in the laboratory in order to understand geologic history of Mars. According to the Meteoritical Bulletin Database, there are 197 approved martian meteorites in our collection, composed mainly of shergottites, with minor contribution from nakhlites and chassignites.

Here, we report spatially resolved FTIR spectroscopy of a total of 12 grains from 4 martian meteorites, ALHA 84001 (orthopyroxenite), Chassigny (chassignite), Nakhla (nakhlite), and EETA 79001 (shergottite). In addition to their mid-infrared spectra, chemical distribution images of silicates, aliphatic hydrocarbons, and OH content were generated for all grains with  $\sim 1 \mu\text{m}$  spatial resolution.

## 2. MATERIALS and METHODS

We have received small chips of meteorites from the Smithsonian Institution (SI) as well as NASA's Johnson

\* Sorumlu yazar (Corresponding Author)  
e-mail : myesiltas@knights.ucf.edu

Space Center (JSC) (Table 1). The chips were ground down to powder size in the laboratory. FTIR imaging experiments were conducted at the Synchrotron Radiation Center, University of Wisconsin in Madison, using the IRENI (InfraRed Environmental Imaging) synchrotron beamline [14]. In IRENI, a matrix of rays from 12 synchrotron beams was arranged to illuminate the sample under the microscope. This arrangement results much brighter light source than conventional thermal light sources, which then homogeneously illuminate 4096 pixels of the commercial focal plane array (FPA) detector. A Bruker Hyperion 3000 IR microscope with a 74X magnification objective was coupled to a Bruker Vertex 70 FTIR spectrometer for our infrared measurements and a condenser of 0.60 numerical aperture was used to match the aperture of the objective, which corresponds to a pixel size of  $0.54 \mu\text{m} \times 0.54 \mu\text{m}$ . Infrared spectra were collected in the  $4000\text{--}850 \text{ cm}^{-1}$  with  $4 \text{ cm}^{-1}$  spectral resolution and 128 scans were co-added. Before each measurement, a sample-free region of the diamond window was used for the collection of reference spectrum.

**Table 1.** Samples investigated in this work.

Meteorite Name	Type	Source
EET A79001	Shergottite	JSC
Nakhla	Nakhlite	SI
Chassigny	Chassignite	SI
ALH 84001	Orthopyroxenite	JSC

### 3. RESULTS AND DISCUSSION

Results show that  $1180\text{--}850 \text{ cm}^{-1}$  region in the spectra of EET A79001 and ALH 84001 contains three peaks at  $1043, 942,$  and  $878 \text{ cm}^{-1}$ , which can be attributed to Si-O stretching vibrations in silicates. These peaks appear more prominent and at  $\sim 20 \text{ cm}^{-1}$  higher frequencies in the spectra of Nakhla. While it is a single peak in others, the peak near  $878 \text{ cm}^{-1}$  is a doublet in the spectra of Nakhla with positions of  $918 \text{ cm}^{-1}$  and  $878 \text{ cm}^{-1}$ . Based on the infrared spectra, Chassigny appears to have a different silicate peak profile than other meteorites studied here, the observed peaks include a shoulder peak near  $1017 \text{ cm}^{-1}$ , a sharp peak at  $965 \text{ cm}^{-1}$  and a broad peak at  $882 \text{ cm}^{-1}$ .

Higher frequency part of the spectra include contribution from organic molecules and OH. Small but sharp peaks at  $2961, 2924,$  and  $2852 \text{ cm}^{-1}$  are due to C-H stretching vibrations in aliphatic moieties. Infrared spectra of most grains present a broad band between  $3750 \text{ cm}^{-1}$  and  $3000 \text{ cm}^{-1}$  due to O-H stretching vibrational modes of adsorbed and/or interlayer water. The spectral region between  $1600\text{--}2600 \text{ cm}^{-1}$  was omitted here because the infrared spectra for the investigated meteorites are featureless in this region.

Infrared images of meteorite grains provide spatial distribution of absorbance at specific wavelengths. These

spatial distribution maps can be useful for the interpretation of relationships of particular functional groups within the local heterogeneity of samples. In other words, relative compositional distribution of organic molecules and mineral species can be obtained, and relative amounts of them can be inferred. In the studied meteorites, silicates appear to be the main component in the grains. Aliphatic hydrocarbons are not present in all grains, however the OH content is present in most grains. The aliphatic and OH content seem to be heterogeneously distributed across the grains (e.g., grains 1 and 2 in ALH 84001 and Chassigny).

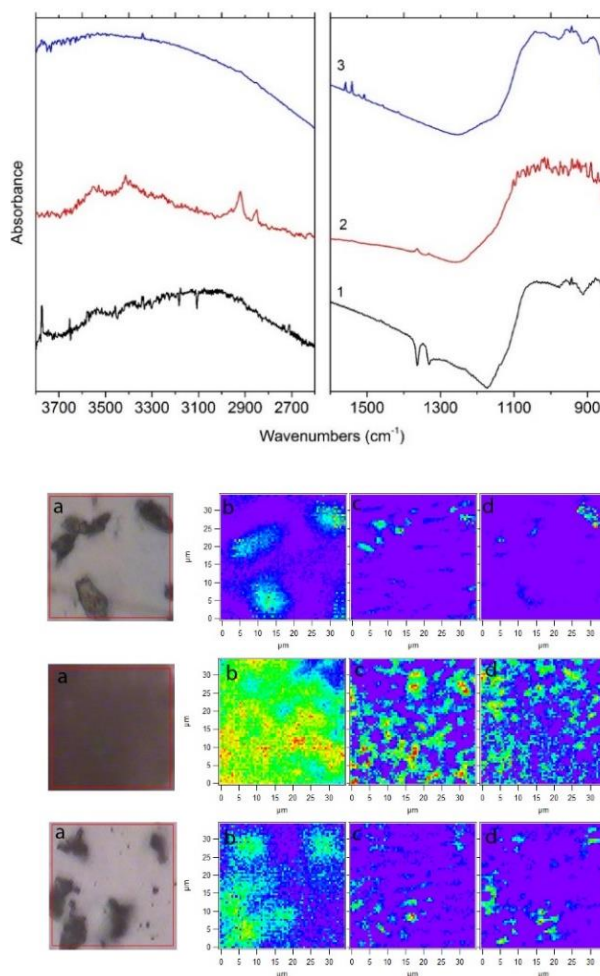


**Figure 1.** Top: Mid-infrared absorbance spectra of EET A79001 grains. Numbers represent different grains in the field of view, and spectra are offset for clarity. Bottom: Visible images of the studied grains (a), spatial distribution of silicates (b,  $1180\text{--}850 \text{ cm}^{-1}$ ), aliphatics (c,  $3000\text{--}2800 \text{ cm}^{-1}$ ), and OH content (d,  $3750\text{--}3000 \text{ cm}^{-1}$ ). Colors of infrared maps indicate absorbance, red being the highest and violet being the lowest. Distribution images from bottom to top correspond to infrared spectra from bottom to top.

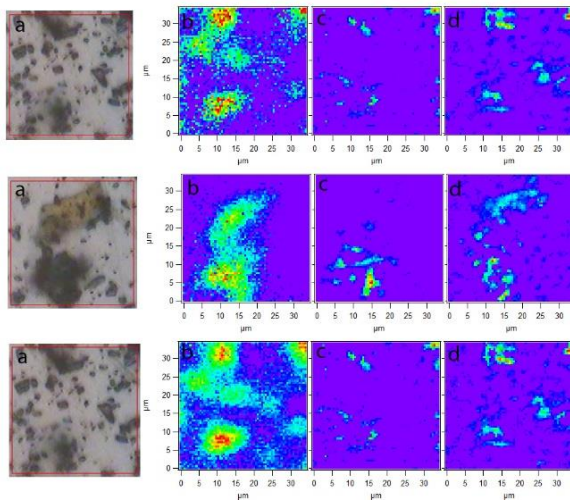
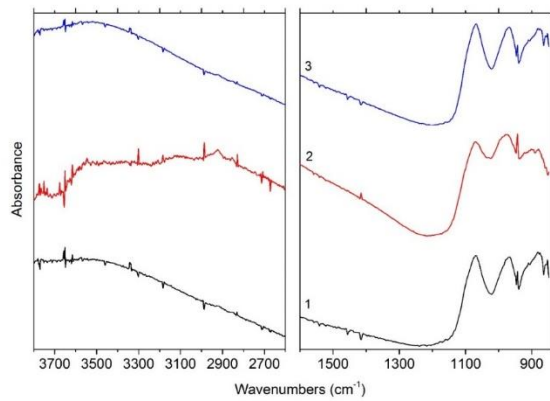


**Figure 2.** Top: Mid-infrared absorbance spectra of Nakhla grains. Numbers represent different grains in the field of view, and spectra are offset for clarity. Bottom: Visible image of the studied grains (a), spatial distribution of silicates (b, 1180–850  $\text{cm}^{-1}$ ), aliphatics (c, 3000–2800  $\text{cm}^{-1}$ ), and OH content (d, 3750–3000  $\text{cm}^{-1}$ ). Colors of infrared maps indicate absorbance, red being the highest and violet being the lowest. Distribution images from bottom to top correspond to infrared spectra from bottom to top.

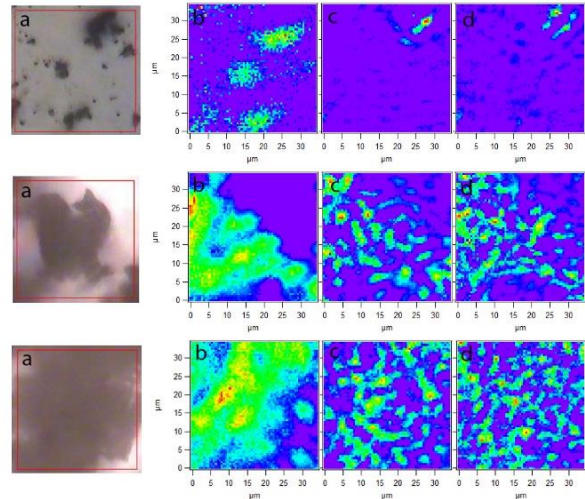
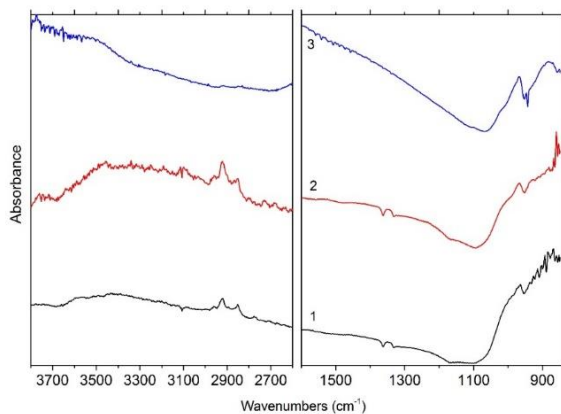


**Figure 3.** Top: Mid-infrared absorbance spectra of Chassigny grains. Numbers represent different grains in the field of view, and spectra are offset for clarity. Bottom: Visible image of the studied grains (a), spatial distribution of silicates (b, 1180–850  $\text{cm}^{-1}$ ), aliphatics (c, 3000–2800  $\text{cm}^{-1}$ ), and OH content (d, 3750–3000  $\text{cm}^{-1}$ ). Colors of infrared maps indicate absorbance, red being the highest and violet being the lowest. Distribution images from bottom to top correspond to infrared spectra from bottom to top.

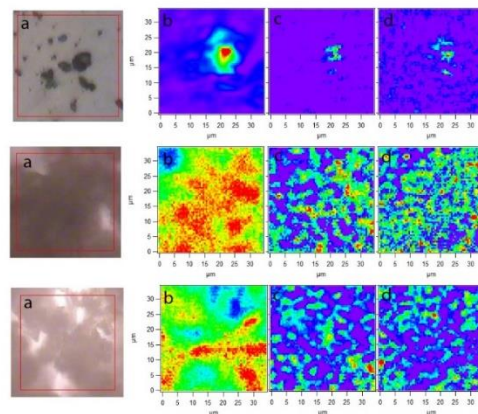
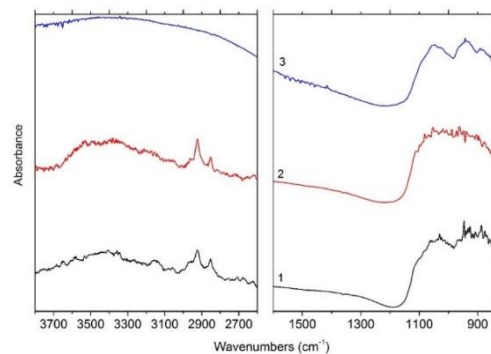


**Figure 4.** Top: Mid-infrared absorbance spectra of ALH 84001 grains. Numbers represent different grains in the field of view, and spectra are

offset for clarity. Bottom: Visible image of the studied grains (a), spatial distribution of silicates (b, 1180–850 cm<sup>-1</sup>), aliphatics (c, 3000–2800 cm<sup>-1</sup>), and OH content (d, 3750–3000 cm<sup>-1</sup>). Colors of infrared maps indicate absorbance, red being the highest and violet being the lowest. Distribution images from bottom to top correspond to infrared spectra from bottom to top.

## 6. CONCLUSION

Spectral investigation of martian meteorites in the infrared may shed light on the mineralogy of Mars, and can also be used to interpret the remote sensing data obtained from orbiters and landers. We presented here that synchrotron-based FTIR spectroscopy can provide invaluable information on meteorites with high resolution. Spectra of the martian meteorites studied here show that some of the grains contain aliphatic type organic moieties as well as OH, although indigeneity of these molecules needs to be confirmed via future experiments. Silicate mineralogy of Chassigny differs from other meteorites presented here. Chassigny was reported to be olivine-rich meteorite with regions of olivine + pyroxene combinations [15]. We believe silicate peaks in the spectra of Chassigny show infrared features due to both olivine and pyroxene, in agreement with [15]. We note that slight spectral differences for each meteorite may be attributed to orientation effects in the crystal structure of minerals. ALH 84001 is an orthopyroxenite meteorite, meaning that the mineralogy is dominated by the mineral orthopyroxene, and the differences in the spectra of this meteorite may be partially due to pyroxene minerals of different compositions (e.g., high-Ca vs. low-Ca pyroxenes). Spatial distribution maps present that aliphatic moieties and OH are distributed heterogeneously, indicating complex parent body processes.

## ACKNOWLEDGEMENT

We thank SI and NASA's JSC for providing the meteorite samples. IRENI beamline's construction and development was supported by NSF MRI award # 0619759.

## REFERENCES

- [1] Bridges J. C. & Warren P. H., "The SNC meteorites: basaltic igneous processes on Mars", *Journal of the Geological Society*, 163:229–251, (2006).
- [2] Fritzi J., Artemieva N., and Greshake A., "Ejection of Martian meteorites", *Meteoritics & Planetary Science*, 40:1393–1411 (2005).
- [3] Treiman A. H., Gleason J. D., and Bogard D. D., "The SNC meteorites are from Mars", *Planetary and Space Science*, 48:1213–1230, (2000).
- [4] McKay D. S., Gibson E. K., Jr., Thomas-Keptra K. L., Vali H., Romanek C. S., Clemett S. J., Chillier X. D. F., Macchling C. R., and Zare R. N., "Search for past life on Mars: Possible relic biogenic activity in Martian meteorite ALH 84001", *Science*, 273:924–930. (1996).
- [5] Steele A., Fries M. D., Amundsen H. E. F., Mysen B. O., Fogel M. L., Schweizer M., Boctor N. Z., "Comprehensive imaging and Raman spectroscopy of carbonate globules from Martian meteorite ALH 84001 and a terrestrial analogue from Svalbard", *Meteoritics & Planetary Science*, 42:1549–1566, (2007).
- [6] Lane M. D., Dyar M. D., and Bishop J. L., "Spectroscopic evidence for hydrous iron sulfate in the Martian soil", *Geophysical Research Letters*, 31:L19702, (2004).
- [7] Altheide T. S., Chevrier V. F., Dobreá E. N., "Mineralogical characterization of acid weathered phyllosilicates with implications for secondary martian deposits", *Geochimica et Cosmochimica Acta*, 74:6232–6248, (2010).
- [8] Dyar M. D., Treiman A. H., Pieters C. M., Hiroi T., Lane M. D., and O'Connor V., "MIL03346, the most oxidized Martian meteorite: A first look at spectroscopy, petrography, and mineral chemistry", *Journal of Geophysical Research*, 110:E09005, (2005).
- [9] Ehlmann B. L. and Edwards C. S., "Mineralogy of the Martian Surface", *Annu. Rev. Earth Planet. Sci.*, 42:291–315, (2014).
- [10] Stephen N. R., Schofield P. F., Berry A. J., and Donaldson P., "Mid-IR Mapping of Martian Meteorites; Spatially Resolved Mineral Spectra from a Synchrotron Source", *45th Lunar and Planetary Science Conference*, #1378, (2014).
- [11] Stephen N. R., Schofield P. F., Berry A. J., "Infrared mapping of silicate minerals in Martian meteorites using a synchrotron light source", *EPSC Abstracts*, 8:297, (2013).
- [12] Anderson M. S., Andringa J. M., Carlson R. W., Conrad P., Hartford W., Shafer M., Soto A., and Tsapin A. I., "Fourier transform infrared spectroscopy for Mars science", *Review of Scientific Instruments*, 76:034101, (2005).
- [13] Yesiltas M. and Kebukawa Y., "Associations of organic matter with minerals in Tagish Lake meteorite via high spatial resolution synchrotron-based FTIR microspectroscopy", *Meteoritics & Planetary Science*, 51: 584–595, (2016).
- [14] Nasse M. J., Mattson E. C., Reiningger R., Kubala T., Janowski S., El-Bayyari Z. and Hirschmugl C. J., "Multi-beam synchrotron infrared chemical imaging with high spatial resolution: Beam line realization and first reports on image restoration", *Nuclear Instruments & Methods in Physics Research Section a-Accelerators Spectrometers Detectors and Associated Equipment*, 649:172–176, (2011).
- [15] Storrie-Lombardi M. C., Muller J. P., Fisk M. R., Griffiths A. D., and Coates A. J. "Potential for non-destructive astrochemistry using the ExoMars PanCam", *Geophysical Research Letters*, 35: L12201, doi:10.1029/2008GL034296, (2008).